Check for updates

The Influence of Navigation and Remote Sensing LEO Satellite Attitude on BDS Augmentation

Li Tian[1,2](✉), Wei Zhang[1,2], Shuangna Zhang[2], and Qijia Dong[2]

[1] Tianjin Zhong Wei Aerospace Data System Technology Co., Ltd., Tianjin 300301, China
[2] Space Star Technology Co., Ltd., Beijing 100086, China

Abstract. In remote sensing tasks, LEO satellites need to adjust the attitude. The influence of the LEO satellite attitude on the augmentation of BDS is researched. In the paper, an on-orbit test scenario is built based on MATLAB and STK simulation software. The number and PDOP values of BDS satellites received by the LEO satellite receiver are analyzed under the three common satellite attitudes of LEO satellites: stable coordinate axis, cruising to the sun, and staring at the target area. In addition, a LEO satellite on ascending orbit and descending orbit was evaluated for two times. The results show that in the telemetry mission, the LEO satellite passes through the same target area, and the satellite attitude has a greater impact on the LEO satellites receiver to receive BDS satellites. Comparing the simulation data with the on-orbit telemetry data, the satellite receiver receives the BDS satellites basically the same, which verifies the reliability of the simulation data and provides support and reference for the on-orbit test.

Keywords: LEO satellite · BDS augmentation · Satellite attitude

1 Introduction

The satellite navigation system as an important national space infrastructure can provide any weather, any time, high-precision positioning, navigation and timing services. It occupies an increasingly important position in the field of national defense and the national economy. Navigation and remote sensing are the most important applications of civil satellites, and they are also an important part of our country's space-based information system. The two are different in constellation configurations, signal structures, and application modes, so that it is difficult to achieve complete integration. LEO satellite serves as the supplement and backup of the current four major satellite navigation systems (GPS, GLONASS, BDS and Galileo). It is in a stage of rapid development, providing development space for navigation and synesthesia integration.

The orbital height of LEO satellites is 500–2000 km. The LEO satellites, compare with medium and high orbit satellites are lighter in weight and lower in orbit. They can be launched by multiple satellites with one arrow. The research and development costs of satellites and rocket launch costs are lower. The LEO satellites have high ground dynamics, downlink wireless signal Doppler is large, and navigation signals have fast

© ICST Institute for Computer Sciences, Social Informatics and Telecommunications Engineering 2021
Published by Springer Nature Switzerland AG 2021. All Rights Reserved
X. Wang et al. (Eds.): AICON 2021, LNICST 396, pp. 138–152, 2021.
https://doi.org/10.1007/978-3-030-90196-7_13

ambiguity resolution and convergence. It is suitable for fast positioning and precision augmentation of navigation on the ground. In addition, the LEO satellites are close to the ground, suitable for the detection and information acquisition of the earth and celestial bodies, data transmission assistance, and remote sensing data analysis and processing, and can perform fine synthesizing detection of ground targets.

At present, the LEO navigation augmentation technology has become a hot direction of research institutions at home and abroad. Design the LEO navigation to enhance satellite constellation, and give the results that the influence of the constellation configuration, orbit height, and orbit inclination on the ground coverage. The LEO satellites combine with GNSS can improve the geometric accuracy [1, 2]. The new constellation configuration design proposed [3]. A LEO satellite navigation augmentation system with integrated communication and navigation is designed, which is based on LEO communication technology to achieve navigation augmentation [4]. The analysis of the attitude control of the remote sensing satellite telemetry mission is analyzed, but did not analyze the impact on the navigation performance [5–7]. There is no article for analyzing the influence that the attitudes of the LEO satellite in the remote sensing mission affect the navigation and positioning. Orienting to engineering, this article analyzes that the influence of navigation and remote sensing integrated LEO satellite attitude on BDS augmentation.

2 Navigation and Remote Sensing LEO Satellite Augmentation System

2.1 Features and Research Goals of Navigation and Remote Sensing LEO Satellite

At present, remote sensing satellites are developing in the direction of LEO satellites. Satellite navigation and positioning are the basis for remote sensing data analysis and calibration, such as remote sensing satellite positioning and remote sensing target positioning. LEO satellites are close to the ground and have a finer remote sensing resolution compared with medium-high orbit satellites. The following Table 1 gives a summary. However, in the process of telemetry missions, the satellite attitude is in a maneuvering state, which has a greater impact on the satellite receivers to receive BDS satellites. It is showed by Table 1.

In the remote sensing tasks, LEO satellite integrated with navigation and remote has the phenomenon of adjusting its attitudes. The LEO satellite attitudes will have a certain impact on the number of BDS satellites received by the satellite receiver. On the one hand, the LEO satellite attitudes affect the orbit determination performance. Due to the satellite attitude adjustment, the receiver channel frequently changes satellites, which affects the positioning accuracy. On the other hand, the LEO satellite attitudes affect the augmentation capabilities of users. Because the satellite transmitter broadcasts the effective ephemeris of the BDS satellites visible to the satellite receiver, and the LEO satellite attitude affects the generation of the effective ephemeris. In this paper, LEO satellite attitudes including stable coordinate axis, cruising to the sun, and staring at the target area, have an effect on satellites receiver to receive BDS satellites and PDOP values. It can support the on-orbit test.

Table 1. Comparison of medium, high and low orbit satellites.

System type		Resolution
GEO remote sensing satellite	U.S. meteorological satellite GOES	Kilometer level
	Europe GEO-Oculus	Meter level
	China GF-4	Optical imaging 50 m
HEO remote sensing satellite	Electronic weather satellite	Kilometer level
	Amber 4K remote sensing satellite	Meter level
MEO remote sensing satellite	U.S. 8X satellite	Optical imaging SAR 1 m
	French MEO satellite	Optical imaging SAR 1 m
LEO remote sensing satellite	KH-12	Optical imaging SAR 1 m
	Lacrosse	Microwave SAR 0.3 m
	GF-2	Optical imaging SAR 0.8 m
	GF-3	Microwave SAR 1 m

2.2 System Composition

The system is mainly composed of BDS satellites, navigation and remote sensing integrated LEO satellite, and users. The remote sensing integrated LEO satellite includes a satellite receiver, satellite BDS signal receiving antenna, a satellite transmitter, and satellite transmitting antenna. It is showed by Fig. 1.

The receiver receives the BDS satellite signal through the receiving antenna, and performs orbit prediction and clock error prediction based on BDS observation data and navigation messages. The satellite transmitter receives orbit forecast and clock error forecast results, and generates LEO navigation augmentation information. The IF module in the satellite transmitter modulates the pseudo code and enhanced information to generate an intermediate frequency signal. The RF module in the satellite transmitter is up-converted, and the intermediate frequency signal is generated into the RF signal. Then the satellite transmitter sends to users via telemetry antenna. The clock module is used for time synchronization between the satellite receiver and t the satellite transmitter.

The workflow figure is showed by Fig. 2.

2.3 Satellite Attitudes

The satellite attitudes are the direction of the space when it is moving on the orbit. The satellite attitudes are represented by three variables: yaw, roll and pitch in the orbital coordinate system. The origin O (x_0, y_0, z_0) of the orbital coordinate system is located on the satellite. The Z_0 axis points to the center of the earth, which is the yaw direction. The X_0 axis is along the tangential direction of the track surface and is perpendicular to the Z_0 axis, which is the rolling direction. The Y_0 axis is perpendicular to the track surface and forms a right-handed system with the X_0 axis and Y_0 axis, which is the pitch

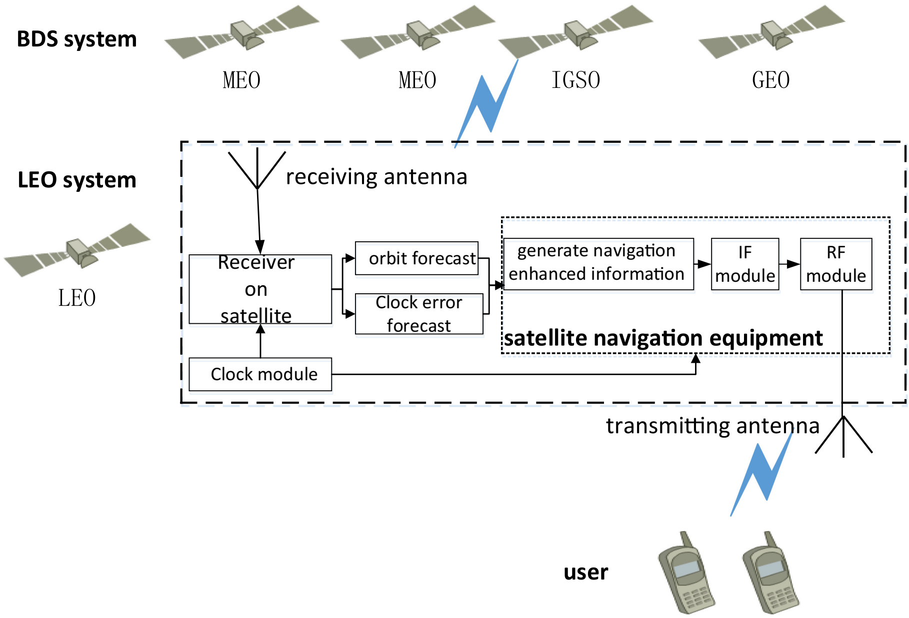

Fig. 1. Navigation and remote sensing LEO satellite augmentation system

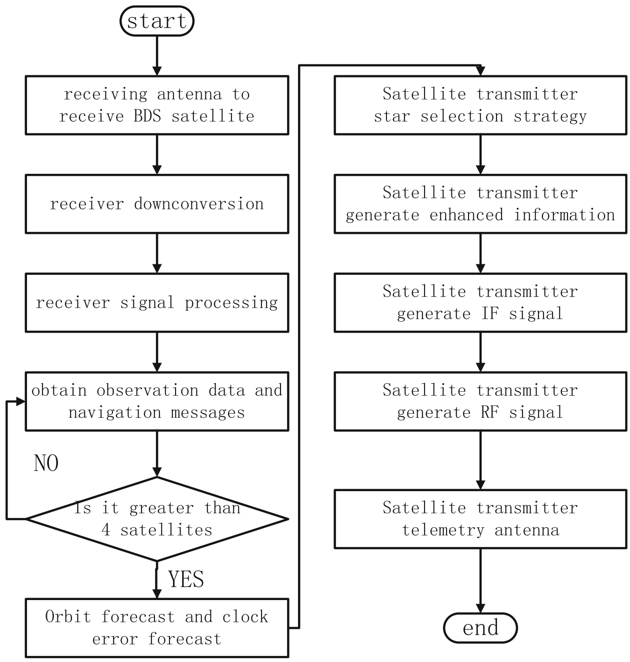

Fig. 2. LEO with navigation and remote integrated enhanced BDS system.

direction. Yaw (pitch) refers to the attitude angle of rotation around the z axis. Roll refers to the attitude angle of rotation around the x-axis. Pitch (yaw) refers to the attitude angle of rotation around the y-axis. Show in the Fig. 3 below.

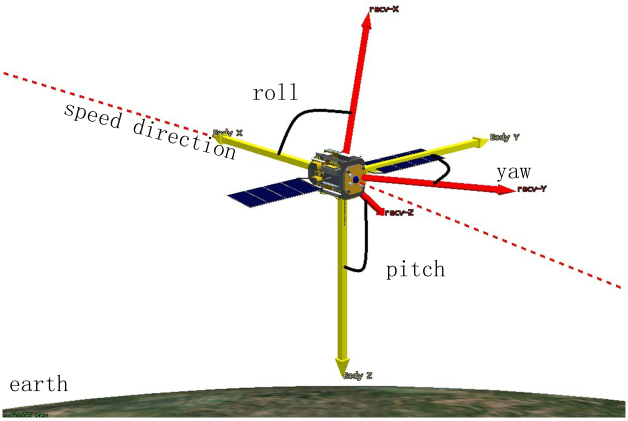

Fig. 3. Satellite attitudes diagram.

With the gradual deepening of the exhibition of remote sensing technology applications, satellite will adopt different attitude modes according to the tasks performed during orbit, such as stable coordinate axis, cruising to the sun, and s staring at the target, etc.

The mode of staring at the target has become one common attitude of remote sensing satellites, which enables the satellite platform to continuously observe hotspot areas. In this attitude mode, the ground station adjusts the satellite attitude. A coordinate axis of the imaging system or optical axis of optical load on the satellite platform always point to the targets. So as to continuously obtain the dynamic information of the target area, it has high engineering application value. Show in the Fig. 4 below.

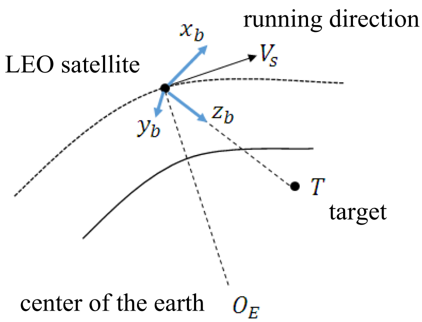

Fig. 4. Staring at the target schematic diagram.

The mode of stable coordinate axis is a stable attitude relative to the spin of the satellite. It means that the satellite body is stable in the three directions of X, Y, and Z, and maintains a certain attitude relationship with the earth. This attitude adapts to most satellite applications, easy to meet the directional requirements of the payload, and easy to achieve orbit control. In the orbital plane of LEO, the $+Z_0$ axis direction always points to the center of the earth, and the $+X_0$ axis direction is along the forward tangential direction. Show in the Fig. 5 below.

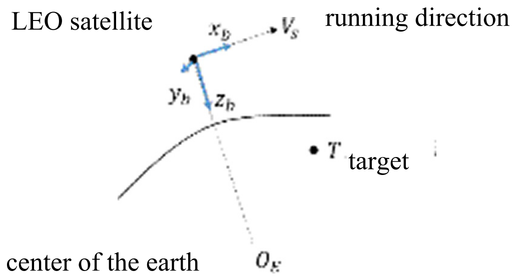

Fig. 5. Stable coordinate axis schematic diagram.

Cruising to the sun is one of the commonly used attitude control mission modes for satellites. It sets the desired attitude of the satellite so that the solar array plane of the satellite is fully aligned with the sun to provide sufficient energy. For example, the +z0 axis of the low-orbit satellite points to the sun. Show in the Fig. 6 below.

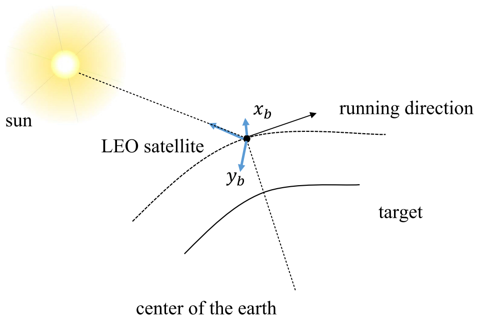

Fig. 6. Cruising to the sun schematic diagram.

3 System Simulation and Verification

3.1 Verification Scenario

In order to verify the influence of navigation and remote sensing LEO satellite attitude on BDS augmentation, a test verification platform was built based on MATLAB and

Table 2. LEO satellite attitude.

Number	LEO satellite attitude	Detailed settings
1	Staring at the targets	$+Z_0$ axis stares at Beijing
2	Stable coordinate axis	$+Z_0$ axis always points to the center of the earth; $-X_0$ axis is along the tangential direction of advancement
3	Orienting toward the sun	$-Y_0$ axis orients to the sun

STK software. The BDS system is the BD3 in orbit. The ground station is Beijing. And the orbital height of the LEO satellite is 500 km. The LEO satellite attitude is shown in the Table 2.

STK software simulates the above 3 types of attitudes scenarios are as follows in the Fig. 7:

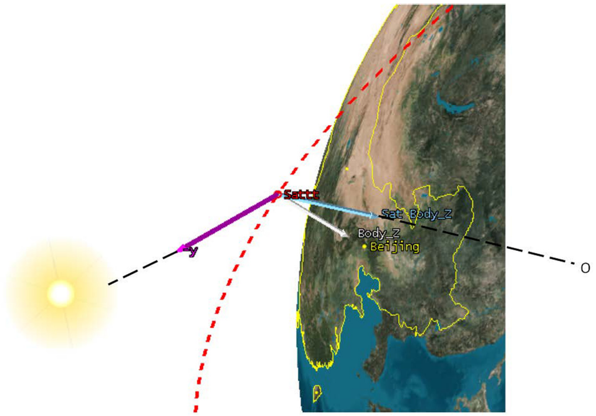

Fig. 7. LEO satellite 3 types of attitude schematic diagram.

In different attitudes, the sensitivity of the satellite receiver is −163 dBW. The receiving antenna is installed at the same position on the satellite, and it points differently as the satellite attitude changes. For example, when the satellite is in a stable coordinate axis attitude, the receiving antenna is located −Z axis deviates from −X axis direction 30° in the satellite body coordinate system.

The return period of the satellite is about 24 h, and the simulation time is selected as 2020.8.31 00:00:00-2020.09.01 04:00:00. There are 6 time periods when the LEO satellite transits the target area of Beijing, as shown in the following Table 3:

The trajectory of LEO satellite includes ascending orbit and descending orbit. The orbits numbered 1, 2, 5, and 6 are satellite ascending orbits, and this orbit is the process from low latitude to high latitude. The orbits numbers 3 and 4 are the descending orbit, and this orbit is the process from high latitude to low latitude. Select 2 sets of ascending orbits (No. 1 and No. 2) and 2 sets of descending orbits (No. 3 and No. 4) to analyze the performance of navigation and remote sensing LEO satellite attitude on BDS augmentation.

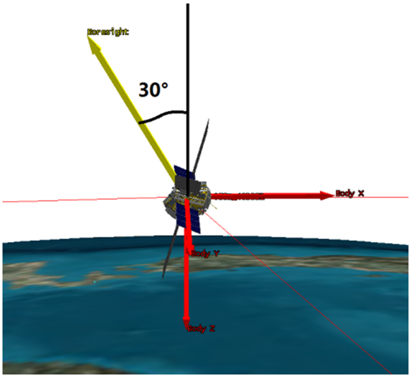

Fig. 8. The relationship between antenna pointing and satellite body coordinate system.

Table 3. LEO and target area Beijing visible time.

Number	Visible time	Visible length of time
1	2020-8-31 09.06.07-09:17:30	682
2	2020-8-31 10:40:35-10:49:17	522
3	2020-8-31 19:42:49-19.53.20	631
4	2020-8-31 21:16:12-21:26:57	645
5	2020-9-1 08:44:42-08:55:37	654
6	2020-9-1 10:18:32-10:28:35	603

3.2 Validation Results

Under the three attitudes of stable coordinate axis, cruising to the sun, and staring at the target area, LEO satellite passes through the target area of Beijing. The receiving antenna on the LEO satellite receives BDS satellites every 30 s. The number of BDS satellites during the 4 time periods is shown in the following Table 4, 5, 6 and 7. It can be seen that the PDOP value of number of BDS satellites changes with time, as shown in the Figs. 9, 10, 11, 12.

Table 4. Visible satellites in the 1rd period

	Time	Visible satellite PRN		
		Staring at the target area	Stable coordinate axis	Cruising to the sun
1	09.06.07	29.20.43.19.34.32.26.24	23.29.20.43.19.35.34.32.26.25.24	29.20.43.19.34.32.26.24
2	09:06:30	29.20.43.19.34.26.24	23.29.20.43.19.35.34.32.26.25.24	29.20.43.19.34.26.24
3	09:07:00	29.20.43.19.34.26.24	23.29.20.43.19.35.34.32.26.25.24	29.20.43.19.34.26.24
4	09:07:30	29.20.43.19.34.26.25.24	23.29.20.43.19.35.34.32.26.25.24	29.20.43.19.34.26.25.24
5	09:08:00	29.20.43.19.34.26.25.24	23.29.20.43.19.35.34.32.26.25.24	29.20.43.19.34.26.25.24
6	09:08:30	29.20.43.19.34.25.24	23.29.20.43.19.35.34.32.26.25.24	29.21.20.43.19.34.26.25.24
7	09:09:00	29.20.43.19.34.25.24	23.29.20.43.19.35.34.32.26.25.24	29.21.20.43.19.34. 25.24
8	09:10:30	29.21.20.43.19.34.25.24	23.29.20.43.19.35.34.32.26.25.24	29.21.20.43.19.34.25.24
9	09:11:00	29.21.20.43.19.34.25.24	29.20.43.19.35.34.32.26.25.24	29.21.20.43.19.34.25.24
10	09:11:30	29.21.20.43.19.34.25.24	29.20.43.19.35.34.32.26.25.24	29.21.20.43.19.34.25.24
11	09:12:00	29.21.20.43.19.34.25.24	29.20.21.43.19.35.34.32.26.25.24	29.21.20.43.19.34.25.24
12	09:12:30	29.21.20.43.19.34.25.24	29.20.21.43.19.35.34.32.26.25.24	29.21.20.43.19.34.25.24
13	09:13:00	29.21.20.43.19.34.25.24	29.20.21.43.19.35.34.32.26.25.24	29.21.20.43.19.34.25.24
14	09:13:30	29.21.20.43.19.34.25.24	29.20.21.43.19.35.34.32.26.25.24	29.21.20.43.19.34.25.24
15	09:14:00	29.21.20.43.19.34.25.24	29.20.21.43.19.35.34.32.26.25.24	29.21.20.43.19.34.25.24
16	09:14:30	29.21.20.43.19.34.25.24	29.20.21.43.19.35.34.26.25.24	29.21.20.43.19.34.25.24
17	09:15:00	29.21.20.43.19.34.25.24	29.20.21.43.19.35.34.26.25.24	29.21.20.43.19.34.25.24
18	09:15:30	29.21.20.43.19.34.25.24	29.20.21.43.19.35.34.26.25.24	29.21.20.43.19.34.25.24
19	09:16:00	29.21.20.43.19.34.25.24	29.20.21.43.19.35.34.26.25.24	29.21.20.43.19.34.25.24
20	09:16:30	29.21.20.43.19.34.25.24	29.20.21.43.19.35.34.26.25.24	29.21.20.46.43.19.34.25.24
21	09:17:00	29.21.20.46.43.19.34.25.24	29.20.21.43.19.35.34.26.25.24	29.21.20.46.43.19.34.25.24
22	09:17:30	29.21.46.43.19.34.25.24	29.20.21.43.19.35.34.26.25.24	29.21.20.43.19.34.25.24
23	09:10:30	29.21.46.43.19.34.25.24	29.20.21.43.19.35.34.26.25.24	29.21.20.43.19.34.25.24

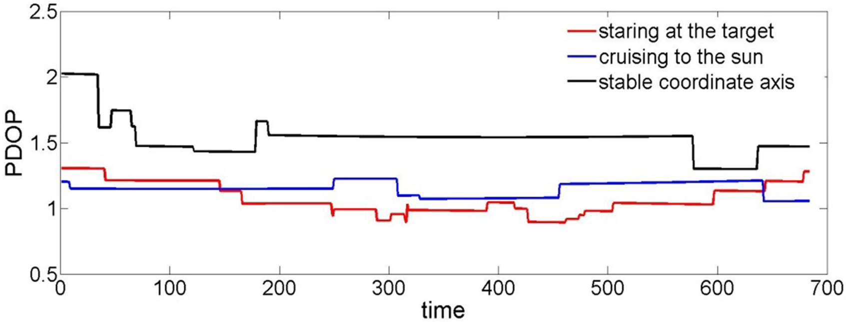

Fig. 9. Visible BDS satellite PDOP value in the 1rd period.

Table 5. Visible satellites in the 2rd period

	Time	Visible satellite PRN		
		Staring at the target area	Stable coordinate axis	Cruising to the sun
1	10:40:35	23.21.20.43.19.35.34.26	23.21.20.44.43.19.37.35.34.26.24	23.21.20.43.19.35.34.26
2	10:41:00	23.21.20.43.19.35.34.26	23.21.20.44.43.19.37.35.34.26.24	23.21.20.43.19.35.34.26
3	10:41:30	23.21.20.43.19.35.34.26	23.21.20.44.43.19.37.35.34.26.24	23.21.20.43.19.35.34.26
4	10:42:00	23.21.43.19.35.34.26	23.21.20.44.43.19.37.35.34.26.24	23.21.43.19.35.34.26
5	10:42:30	23.21.43.19.35.34.26.24	23.21.20.44.43.19.37.35.34.26.24	23.21.43.19.35.34.26.24
6	10:43:00	23.21.43.19.35.34.26.24	23.21.20.44.43.19.37.35.34.26.24	23.21.43.19.35.34.26.24
7	10:43:30	23.21.43.19.35.34.26.24	23.21.20.44.43.19.37.35.34.26.24	23.21.43.19.35.34.26.24
8	10:44:00	21.43.19.35.34.26.24	23.21.20.44.43.19.37.35.34.26.24	21.43.19.35.34.26.24
9	10:44:30	22.21.43.19.35.34.26.24	23.21.20.44.43.19.37.35.34.26.24	22.21.43.19.35.34.26.24
10	10:45:00	22.21.43.19.35.34.26.24	23.21.20.44.43.19.35.34.26.24	22.21.43.19.35.34.26.24
11	10:45:30	22.21.43.19.35.34.26.24	23.21.20.44.43.19.35.34.26.24	22.21.43.19.35.34.26.24
12	10:46:00	22.21.43.19.35.34.26.24	23.21.20.44.43.19.35.34.26.24	22.21.43.19.35.34.26.24
13	10:46:30	22.21.43.19.35.34.26.24	23.22.21.20.44.43.19.35.34.26.24	22.21.43.19.35.34.26.24
14	10:47:00	22.21.43.19.35.34.26.24	23.22.21.20.44.43.19.35.34.26.24	22.21.43.19.35.34.26.24
15	10:47:30	22.21.43.19.35.34.26.24	23.22.21.20.44.43.19.35.34.26.24	22.21.43.19.35.34.26.24
16	10:48:00	22.21.43.19.35.34.26.24	23.22.21.20.44.43.19.35.34.26.24	22.21.43.19.35.34.26.24
17	10:48:30	22.21.43.19.35.34.26.24	23.22.21.20.44.43.19.35.34.26.24	22.21.43.19.35.34.26.24
18	10:49:00	22.21.43.19.35.34.26.24	23.22.21.44.43.19.35.34.26.24	22.21.43.19.35.34.26.24

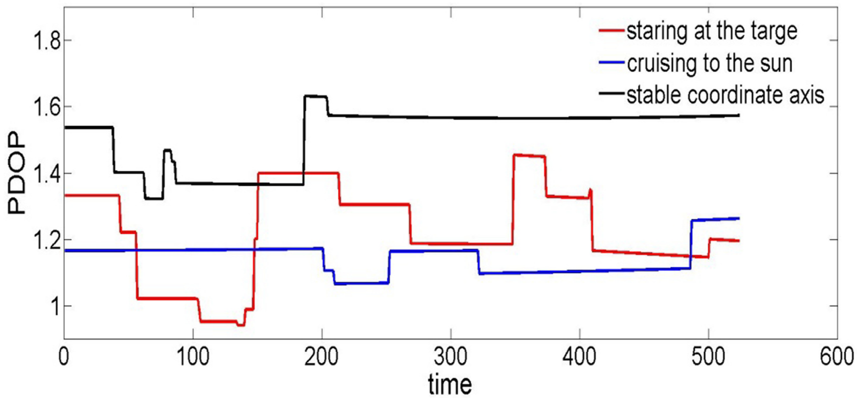

Fig. 10. Visible BDS satellite PDOP value in the 2rd period.

Table 6. Visible satellites in the 3rd period

	Time	Visible satellite PRN		
		Staring at the target area	Stable coordinate axis	Cruising to the sun
1	19:43:00	23.42.41.33.26.24	23.22.28.27.44.42.41.35.33.32.26.24	23.42.41.33.26.24
2	19:43:30	23.42.41.33.26.24	23.22.28.27.44.42.41.35.33.32.26.24	23.42.41.33.26.24
3	19:44:00	23.42.41.33.26.24	23.22.28.27.44.42.41.35.33.32.26.24	23.42.41.33.26.24
4	19:44:30	23.42.41.33.26.24.25	23.28.27.44.42.41.35.33.32.26.24	23.42.41.33.26.25.24
5	19:45:00	23.42.41.33.26.24.25	23.28.27.44.42.41.35.33.32.26.24	23.42.41.33.26.25.24
6	19:45:30	23.42.41.33.26.24.25	23.28.27.44.42.41.35.33.32.26.24	23.42.41.33.26.25.24
7	19:46:00	23.42.41.33.26.24.25	23.28.27.44.42.41.35.33.32.26.24	23.42.41.33.26.25.24
8	19:46:30	23.42.41.33.26.24.25	23.30.28.27.44.42.41.35.33.32.26.24	23.42.41.33.26.25.24
9	19:47:00	23.42.41.33.26.24.25	23.30.28.27.44.42.41.35.33.32.26.24	23.42.41.33.26.25.24
10	19:47:30	23.42.41.33.26.24.25	23.30.28.27.44.42.41.35.33.32.26.24	23.42.41.33.26.25.24
11	19:48:00	23.42.41.33.26.24.25	23.30.28.27.44.42.41.35.33.32.26.24	23.42.41.33.26.25.24
12	19:48:30	23.42.41.33.26.24.25	23.30.28.27.42.41.33.32.26.24	23.42.41.33.26.25.24
13	19:49:00	42.41.33.26.24.25	23.30.28.27.42.41.33.32.26.24	42.41.33.26.25.24
14	19:49:30	42.41.33.26.24.25	23.30.28.27.42.41.33.32.26.24	42.41.33.26.25.24
15	19:50:00	42.41.33.26.24.25	23.30. 27.42.41.33.32.26.24	42.41.33.26.25.24
16	19:50:30	42.41.33.26.24.25	23.30. 27.42.41.33.32.26.24	42.41.33.26.25.24
17	19:51:00	41.33.32.26.24.25	23.30. 27.42.41.33.32.26.24	41.33.32.26.25.24
18	19:51:30	41.33.32.26.24.25	23.30. 27.42.41.33.32.26.24	41.33.32.26.25.24
19	19:52:00	41.33.32.26.24.25	23.30. 27.42.41.33.32.26.24	41.33.32.26.25.24
20	19:52:30	41.33.32.26.24.25	23.30. 27.42.41.33.32.26.24	41.33.32.26.25.24

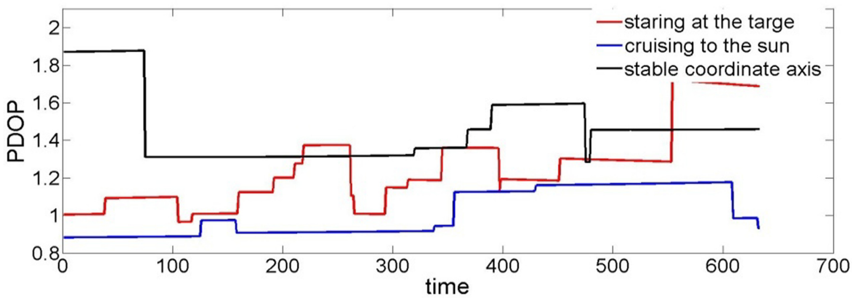

Fig. 11. Visible BDS satellite PDOP value in the 3rd period.

Table 7. Visible satellites in the 4rd period

	Time	Visible satellite PRN		
		Staring at the target area	Stable coordinate axis	Cruising to the sun
1	21:16:30	23.41.37.33.32.26	23.30.28.27.44.42.41.37.33.32.26	23.41.37.33.32.26
2	21:17:00	23.41.37.33.32.26	23.30.28.27.20.44.42.41.37.33.32.26	23.41.37.33.32.26
3	21:17:30	23.41.37.33.32.26	23.30.28.27.20.44.42.41.37.33.32.26	23.41.37.33.32.26
4	21:18:00	23.41.37.33.32.26	23.30.28.27.20.44.42.41.37.33.32.26	23.41.37.33.32.26
5	21:18:30	23.41.37.33.32.26	23.30.28.27.20.44.42.41.37.33.32.26	23.41.37.33.32.26
6	21:19:00	23.41.37.33.32.26	23.30.28.27.20.44.42.41.37.33.32.26	23.41.37.33.32.26
7	21:19:30	23.41.37.33.32.26	23.30.28.27.20.44.41.37.33.32.26	23.41.37.33.32.26
8	21:20:00	23.41.37.33.32.26.24	23.30.28.27.20.44.41.37.33.32.26	23.41.37.33.32.26.24
9	21:20:30	23.41.37.33.32.26.24	23.30.28.27.20.44.41.37.33.32.26	23.41.37.33.32.26.24
10	21:21:00	23.41.37.33.32.26.24	23.30.28.27.20.44.41.37.33.32.26	23.41.37.33.32.26.24
11	21:21:30	23.41.37.33.32.26.24	23.30.28.27.20.44.41.37.33.32.26	23.41.37.33.32.26.24
12	21:22:00	23.41.37.33.32.26.24	23.30.29.28.27.20.44.41.37.33.32.26	23.41.37.33.32.26.24
13	21:22:30	23.41.37.33.32.26.24	23.30.29.28.27.20.44.41.37.33.32.26	23.41.37.33.32.26.24
14	21:23:00	23.41.37.33.32.26.24	23.30.29.27.20.41.37.33.32.26	23.41.37.33.32.26.24
15	21:23:30	23.41.33.32.26.24	23.30.29.27.20.41.37.33.32.26	23.41.33.32.26.24
16	21:24:00	23.41.33.32.26.24	23.30.29.27.20.41.37.33.32.26	23.41.33.32.26.24
17	21:24:30	23.41.33.32.26.24	23.30.29.27.20.41.37.33.32.26	23.41.33.32.26.24
18	21:25:00	23.41.33.32.26.24	23.30.29.20.41.37.33.32.26	23.41.33.32.26.24
19	21:25:30	23.41.33.32.26.24	23.30.29.20.41.37.33.32.26	23.41.33.32.26.24
20	21:26:00	23.41.32.26.24	23.30.29.20.41.37.33.32.26	23.20.41.32.26.24
21	21:26:30	23.41.32.26.24.20	23.30.29.20.41.37.33.32.26	23.20.41.32.26.24

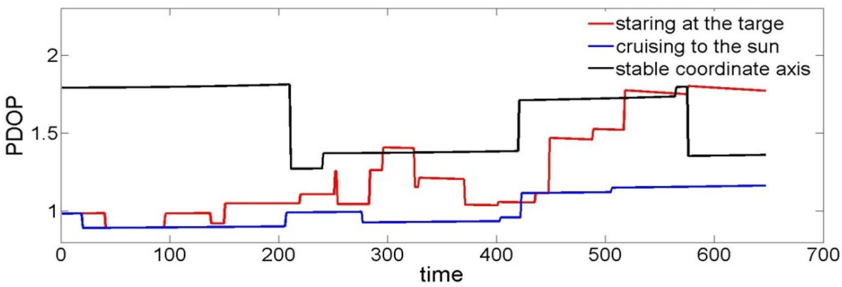

Fig. 12. Visible BDS satellite PDOP value in the 4rd period.

When the LEO satellite is in the ascending orbit through the target area, Table 4 and Table 5 show the PRN of the visible satellites that received by the LEO satellite receiver. When the LEO satellite is in descending orbit through the target area, Table 6 and Table 7 show the PRN of the visible satellites that received by the LEO satellite receiver. From the data in the table, the number of satellites received by the satellite receiver is more than 4, which can achieve positioning. It can be seen that the satellite PRN number is not exactly the same in different attitudes.

Figure 9 and Figure 10 are graphs that show PDOP values of visible satellites received by LEO satellite receiving antenna when the LEO satellite is in the ascending orbit. The simulation results show that the order of the navigation and positioning performance of the LEO satellite from high to low is: staring at the target > cruising to the sun > three-axis stability.

Figure 11 and Figure 12 are graphs that show PDOP values of visible satellites received by LEO satellite receiving antenna when the LEO satellite is in the ascending orbit. The simulation results show that the order of the navigation and positioning performance of the LEO satellite from high to low is: staring at the target > cruising to the sun > three-axis stability.

In summary, when the LEO satellite is in the attitude of staring at the target and orienting toward the sun, the number of BDS satellites is received more. When the LEO satellite is in the attitude of three-axis stable, the number of BDS satellites received by the LEO satellite receiver is small.

4 On-Orbit Evaluation

In order to verify the simulation results, this paper conducts two on-orbit evaluations on a LEO satellite. In order to verify the adequacy of the experiment, the selection target area is visible for a longer period of time, and the satellite trajectory includes ascending orbit and descending orbit. According to the telemetry data of the LEO satellite receiver, the PRN and the number of satellites visible to the satellite receiver are counted and compared with the simulation results (Fig. 13).

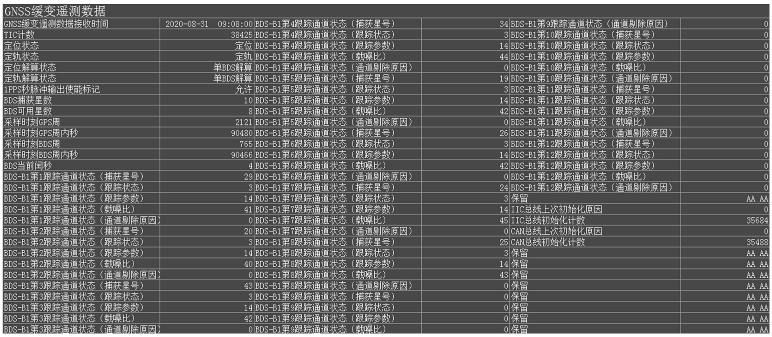

GNSS缓变遥测数据

GNSS缓变遥测数据接收时间	2020-08-31 09:08:00	BDS-B1第4跟踪通道状态（捕获星号）	34	BDS-B1第9跟踪通道状态（通道剔除原因）	0
TIC计数	38425	BDS-B1第4跟踪通道状态（跟踪状态）	3	BDS-B1第10跟踪通道状态（捕获星号）	0
定位状态	定位	BDS-B1第4跟踪通道状态（跟踪参数）	14	BDS-B1第10跟踪通道状态（跟踪状态）	0
定轨状态	定轨	BDS-B1第4跟踪通道状态（载噪比）	44	BDS-B1第10跟踪通道状态（跟踪参数）	0
定位解算状态	单BDS解算	BDS-B1第4跟踪通道状态（通道剔除原因）	0	BDS-B1第10跟踪通道状态（载噪比）	0
定轨解算状态	单BDS解算	BDS-B1第5跟踪通道状态（捕获星号）	19	BDS-B1第10跟踪通道状态（通道剔除原因）	0
1PPS秒脉冲输出使能标记	允许	BDS-B1第5跟踪通道状态（跟踪状态）	3	BDS-B1第11跟踪通道状态（捕获星号）	0
BDS捕获星数	10	BDS-B1第5跟踪通道状态（跟踪参数）	14	BDS-B1第11跟踪通道状态（跟踪状态）	0
BDS可用星数	8	BDS-B1第5跟踪通道状态（载噪比）	42	BDS-B1第11跟踪通道状态（跟踪参数）	0
采样时刻GPS周	2121	BDS-B1第5跟踪通道状态（通道剔除原因）	0	BDS-B1第11跟踪通道状态（载噪比）	0
采样时刻GPS周内秒	90480	BDS-B1第6跟踪通道状态（捕获星号）	26	BDS-B1第11跟踪通道状态（通道剔除原因）	0
采样时刻BDS周	765	BDS-B1第6跟踪通道状态（跟踪状态）	3	BDS-B1第12跟踪通道状态（捕获星号）	0
采样时刻BDS周内秒	90466	BDS-B1第6跟踪通道状态（跟踪参数）	14	BDS-B1第12跟踪通道状态（跟踪状态）	0
BDS当前闰秒	4	BDS-B1第6跟踪通道状态（载噪比）	42	BDS-B1第12跟踪通道状态（跟踪参数）	0
BDS-B1第1跟踪通道状态（捕获星号）	29	BDS-B1第6跟踪通道状态（通道剔除原因）	0	BDS-B1第12跟踪通道状态（载噪比）	0
BDS-B1第1跟踪通道状态（跟踪状态）	3	BDS-B1第7跟踪通道状态（捕获星号）	24	BDS-B1第12跟踪通道状态（通道剔除原因）	0
BDS-B1第1跟踪通道状态（跟踪参数）	14	BDS-B1第7跟踪通道状态（跟踪状态）	3	保留	AA AA
BDS-B1第1跟踪通道状态（载噪比）	41	BDS-B1第7跟踪通道状态（跟踪参数）	14	IIC总线上次初始化原因	0
BDS-B1第1跟踪通道状态（通道剔除原因	0	BDS-B1第7跟踪通道状态（载噪比）	45	IIC总线初始化计数	35684
BDS-B1第2跟踪通道状态（捕获星号）	20	BDS-B1第7跟踪通道状态（通道剔除原因）	0	CAN总线上次初始化原因	0
BDS-B1第2跟踪通道状态（跟踪状态）	3	BDS-B1第8跟踪通道状态（捕获星号）	25	CAN总线初始化计数	35488
BDS-B1第2跟踪通道状态（跟踪参数）	14	BDS-B1第8跟踪通道状态（跟踪状态）	3	保留	AA AA
BDS-B1第2跟踪通道状态（载噪比）	40	BDS-B1第8跟踪通道状态（跟踪参数）	14	保留	AA AA
BDS-B1第2跟踪通道状态（通道剔除原因	0	BDS-B1第8跟踪通道状态（载噪比）	43	保留	AA AA
BDS-B1第3跟踪通道状态（捕获星号）	43	BDS-B1第8跟踪通道状态（通道剔除原因）	0	保留	AA AA
BDS-B1第3跟踪通道状态（跟踪状态）	3	BDS-B1第9跟踪通道状态（捕获星号）	0	保留	AA AA
BDS-B1第3跟踪通道状态（跟踪参数）	14	BDS-B1第9跟踪通道状态（跟踪状态）	0	保留	AA AA
BDS-B1第3跟踪通道状态（载噪比）	42	BDS-B1第9跟踪通道状态（跟踪参数）	0	保留	AA AA
BDS-B1第3跟踪通道状态（通道剔除原因	0	BDS-B1第9跟踪通道状态（载噪比）	0	保留	AA AA

Fig. 13. LEO satellite 3 types of attitude schematic diagram.

Table 8. Visible time of LEO satellite passing through target area Beijing.

Number	Visible time	Visible satellite orienting toward the sun
1	2021-08-31 09:06:56	23.29.20.43.19.35.34.32.26.25.24
2	2021-08-31 09:07:28	23.29.20.43.19.35.34.32.26.25.24
3	2021-08-31 09:08:00	23.29.20.43.19.35.34.32.26.25.24
4	2021-08-31 09:09:04	23.29.20.43.19.35.34.32.26.25.24
5	2021-08-31 09:10:08	23.29.20.43.19.35.34.32.26.25.24
6	2021-08-31 09:11:12	29.20.43.19.35.34.32.26.25.24
7	2021-08-31 09:12:16	29.20.21.43.19.35.34.32.26.25.24
8	2021-08-31 09:13:20	29.20.21.43.19.35.34.32.26.25.24
9	2021-08-31 09:14:24	29.20.21.43.19.35.34.26.25.24
10	2021-08-31 09:15:28	29.20.21.43.19.35.34.26.25.24
11	2021-08-31 09:16:32	29.20.21.43.19.35.34.26.25.24

On August 31, 2020, the LEO satellite is in the ascending orbit. The visible time that LEO satellite passing through the target area was 09:06.07–09:17:30. The time was on the day, and the LEO satellite attitude was cruising to the sun. The telemetry data of the receiver on the LEO satellite is shown in the following Table 8:

On August 31, 2020, the LEO satellite is in the descending orbit. The visible time that LEO satellite passing through the target area was 19:42:49–19:53:20. The time was in the night, and the LEO satellite attitude was three-axis stability. The telemetry data of the receiver on the LEO satellite is shown in the following Table 9:

Table 9. Visible time of LEO satellite passing through target area Beijing.

Number	Visible time	Visible satellite three-axis stability
1	2021-08-31 19:43:56	23.42.41.33.26.24
2	2021-08-31 19:44:28	23.42.41.33.26.24.25
3	2021-08-31 19:45:00	23.42.41.33.26.24.25
4	2021-08-31 19:46:04	23.42.41.33.26.24.25
5	2021-08-31 19:47:08	23.42.41.33.26.24.25
6	2021-08-31 19:48:12	41.33.32.26.24.25
7	2021-08-31 19:49:16	41.33.32.26.24.25
8	2021-08-31 19:50:20	41.33.32.26.24.25
9	2021-08-31 19:51:24	41.33.32.26.24.25
10	2021-08-31 19:52:28	41.33.32.26.24.25

Comparing Table 8 and Table 4, Table 9 and Table 6, the results show that the on-orbit telemetry data is basically the same as the simulation data, except for the low elevation angle and low carrier-to-noise ratio satellites.

The reason for the difference is the complex environment in orbiting space and the influence of ground control satellite attitude maneuverability. The complex environment in orbiting space includes ionosphere and troposphere etc. The simulation results provide support and reference for the on-orbit test.In addition, when there is no telemetry mission it is recommended to use a three-axis stable attitude at night and a cruise attitude toward the sun on the day.

5 Conclusion

This article introduces the composition of the navigation and remote sensing LEO satellite augmentation system. Compare and analyze characteristics of three LEO typical satellite attitudes: staring at the targets, cruising to the sun, and three-axis stability. In order to obtain the simulation data of the influence of navigation and remote sensing LEO satellite attitude on BDS augmentation, a test verification platform is built based on MATLAB and STK software. In the verification platform, the trajectory of LEO satellite includes ascending orbit and descending orbit, the number and the PDOP value of BDS visible satellites received by LEO satellite receiver is verified. Finally, the reliability of the simulation data is verified by on-orbit telemetry data.

References

1. Tian, Y., Zhang, L., Bian, L.: Design of LEO satellites augmented constelliation for navigation. Chinese Space Sci. Technol. **39**(6), 55–61 (2019)
2. Tian, R., Cui, Z., Zhang, S., Wang, D.: Navigation positioning & timing **1**(8), 66–81 (2021)
3. Shen, Y., Zhang, Y.: Design for LEO satellite navigation augmentation system based on integrated communication and navigation. In: Academic Exchange Center of China Satellite Navigation System Management Office. Proceedings of the 11th China Satellite Navigation Annual Conference 2020. LNCS, vol. 9999, pp. 25–29 (2020)
4. Li, Q., Deng, Z., Wang, Y., Wang, J.: Quasi-sun-pointing oriented attitude for solar power satellites. J. Astronaut. **40**(01), 29–40 (2019)
5. Shen, D., Meng, Y., Bian, L.: A global navigation augmentation system based on LEO communication constellation. J. Terahertz Sci. Electron. Inf. Technol. **17**(02), 209–215 (2019)
6. Wang, L., Li, D., Chen, R., et al.: Low earth orbiter (LEO) navigation augmentation: opportunities and challenges. Strat. Study CAE **22**(2), 144–152 (2020)
7. Pan, L., Wang, S., Yuan, J., et al.: Design and simulation of LEO remote sensing satellite. Spacecraft Eng. **30**(01), 52–56 (2021)